Available online at www.sciencedirect.com

ScienceDirect

Ceramics International 40 (2014) 129–140

CERAMICS INTERNATIONAL

www.elsevier.com/locate/ceramint

Structure–property relationships and densification-crystallization behaviours of simplified lithium disilicate glass compositions

Hugo R. Fernandes[a], Dilshat U. Tulyaganov[a,b], Maria J. Pascual[c], José M.F. Ferreira[a,*]

[a]Department of Materials and Ceramics Engineering, CICECO, University of Aveiro, 3810-193 Aveiro, Portugal
[b]Turin Polytechnic University in Tashkent, 17 Niyazova Street, 100095 Tashkent, Uzbekistan
[c]Instituto de Cerámica y Vidrio (CSIC), C/Kelsen 5, Campus de Cantoblanco, 28049 Madrid, Spain

Received 30 April 2013; received in revised form 29 May 2013; accepted 29 May 2013
Available online 4 June 2013

Abstract

The role of each oxide component on the structure of molten glass and on their densification and crystallization behaviours is expected to be more easily assessed for compositions comprising a small number of components. In the present work, binary (Li_2O–SiO_2), ternary (Li_2O–Al_2O_3–SiO_2), and quaternary (Li_2O–K_2O–Al_2O_3–SiO_2) glass compositions were selected. The aim was to investigate the relationships between the compositions and structure of the glasses, namely, the effects of each component on the extent of liquid-in-liquid phase separation, their thermal behaviour and the phase assemblage in the disilicate glass–ceramics. The distribution of structural units in the experimental glasses was assessed using ^{29}Si MAS-NMR spectroscopy. Adding Al_2O_3 played a dual role as network former and modifier when added to the binary system by enhancing Q^2 and diminishing Q^3 structural units. The processing window for sintering, the difference between the onset of crystallisation and glass-transition temperature (T_c−T_g), was too narrow for the less polymerised network structures (binary and ternary systems), hindering the densification of the corresponding glass powder compacts. Oppositly, compositions in the quaternary system featured excellent densification behaviour coupled with high mechanical strength. These features derive from a more rigid glass network comprising four coordinated $(AlO_{4/2})^-$ units and K^+ cations in its vicinity.

Keywords: B. Microstructure-final; C. Thermal properties; D. Glass; D. Glass–ceramics

1. Introduction

The binary alkali silicate glasses may be considered as the original type of all silicate glasses consisting of several components [1–3]. Among the binary alkali silicate glasses the lithia–silica system has gained a great interest for the preparation of glasses and glass–ceramic materials [4–6]. Lithium meta- and di-silicate phases might be formed depending on the SiO_2/Li_2O ratio, presence of nucleating agents, thermal history of parent glasses, *etc.* [7]. The S-shaped path of the melting curve in the Li_2O–SiO_2 system shows that it has to certain extent a tendency to segregation [2]. The glasses with SiO_2 contents higher than the stoichiometric lithium disilicate $Li_2Si_2O_5$ (here after referred as LD) tend to separate into a matrix phase with a composition almost similar to that of LD along with an isolated droplet SiO_2 rich phase, while glasses with Li_2O contents < 30 mol% usually turn out to be opalescent or opaque on cooling owing to phase separation [2]. The composition of the droplet phase tended to a limiting value, *i.e.* towards the disilicate compound that was reached within the Li_2O content of 14–16 mol% in the entire glass, which thereafter remained constant until a composition of 33.3 mol% [2].

The glass–ceramics derived from this parent binary system exhibit some unfavourable characteristics in terms of their mechanical strength and chemical durability which hinder their use in several technological areas. Although chemical durability, which is of major importance for dental materials, has been improved via adding Al_2O_3 and K_2O to stoichiometric LD compositions [8,9], special attention was drawn to non-stoichiometric LD glass–ceramics. The latter have proven to be

*Corresponding author. Tel.: +351 234 370242; fax: +351 234 370204.
E-mail address: jmf@ua.pt (J.M.F. Ferreira).

0272-8842/$ - see front matter © 2013 Elsevier Ltd and Techna Group S.r.l. All rights reserved.
http://dx.doi.org/10.1016/j.ceramint.2013.05.113

Table 1
Compositions of the experimental glasses (mol%).

#	Li_2O–SiO_2			Li_2O–Al_2O_3–SiO_2			Li_2O–K_2O–Al_2O_3–SiO_2		
	A1	A2	A3	B1	B2	B3	C1	C2	C3
Li_2O	26.59	28.09	30.59	26.59	28.09	30.59	22.96	22.96	22.96
K_2O	—	—	—	—	—	—	3.63	5.13	7.63
Al_2O_3	—	—	—	2.63	2.63	2.63	2.63	2.63	2.63
SiO_2	73.41	71.91	69.41	70.78	69.28	66.78	70.78	69.28	66.78
SiO_2/Li_2O	2.76	2.56	2.27	2.66	2.47	2.18	3.08	3.02	2.91

potential candidates for different functional applications due their improved mechanical, chemical and thermal properties [10–15]. It is noteworthy that according to Höland and Beall [7] the term 'non-stoichiometric' implies that SiO_2/Li_2O molar ratio deviates greatly from 2:1 and the system is rendered considerably more complex with numerous additional oxides, including nucleating agents. The introduction of SiO_2-excess to stoichiometric lithium disilicate glass along with additives, such as ZrO_2, Al_2O_3, ZnO, CaO, K_2O, and P_2O_5, has been suggested by Echeverria and Beall [16–18]. Later, P_2O_5 was found to play a crucial role in lithium disilicate transformation and crystallization [19,20]: P_2O_5 (as nucleating agent) at the amount of 1.5–2.5 mol% resulted in glass–ceramics with fine-grained interlocking microstructures, conferring the final products high mechanical strength. A powder processing of lithium disilicate glass–ceramics in a multi-component system with a wide compositional range (in wt%) 57–80 SiO_2, 11–19 Li_2O, 0–13 K_2O, 0–5 Al_2O_3, 0–8 ZnO, 0.1–6, La_2O_3, and 0.1–11 P_2O_5, was thoroughly investigated by Ivoclar-Vivadent company to produce the material IPS Empress®2 [21–24].

In spite of the numerous studies found on non-stoichiometric glasses in the Li_2O–SiO_2 system, compositions with SiO_2/Li_2O molar ratios > 3:1 were scarcely investigated [3,25,26]. We have recently reported on glass compositions with SiO_2/Li_2O molar ratios far beyond that of lithium disilicate stoichiometry [27–31], namely within the range of 3.13–4.88 and containing Al_2O_3 and K_2O, which were compared with a bicomponent glass $23Li_2O$–$77SiO_2$ (mol%) [27,29,30]. The later composition exhibited a cloudy appearance upon cooling while the Al_2O_3 and K_2O containing compositions resulted in transparent glasses due to the presence of Al^{3+}, which acted as network former decreasing the volume fraction and mean diameter of droplet phase. Sintering and crystallization studies of $23Li_2O$–$77SiO_2$ glass powder compacts revealed high fragility, and low flexural strength and density. In contrast, good densification behaviour resulted from adding equimolar amounts of Al_2O_3 and K_2O to the Li_2O–SiO_2 system to obtain the composition $22.96Li_2O$–$2.63Al_2O_3$–$2.63K_2O$–$71.78SiO_2$ (mol%, SiO_2/Li_2O molar ratio of 3.13), and a glass–ceramic with improved mechanical strength [30]. A further insight into the effect of K_2O on structure–property relationships and devitrification behaviour of glasses was made starting from the above referred glass ($22.96Li_2O$–$2.63Al_2O_3$–$2.63K_2O$–$71.78SiO_2$) and adding incremental amounts of K_2O [28,31]. These studies revealed that excess K_2O contents within the range of 2.63–12.63 (mol%) enhanced the liquid–liquid immiscibility as denoted by an increasing of the mean droplet size and their distribution density. On the other hand, increasing K_2O contents resulted in ^{29}Si MAS-NMR spectral changes: decreasing Q^4 units accompanied by an increase of Q^3 units and the appearance a new Q^2 population, suggesting depolymerisation of the silicate glass network, while ^{27}Al MAS-NMR revealed an enhanced role of Al_2O_3 as glass network former. This role implies the association of a cation in the vicinity of each tetrahedral unit in order to maintain local charge neutrality of the $(AlO_{4/2})^-$ units with four bridging oxygens (BO). However, for K_2O/Al_2O_3 molar ratios > 1, there was the formation of a larger fraction of non-bridging oxygens (NBO) due to the excess of K_2O. Additionally K_2O was found to promote surface crystallization in glasses with the predominant formation of lithium metasilicate (LMS) phase. Only in low-K_2O compositions LD was formed, resulting in glass–ceramics with high mechanical strength (~173–224 MPa), good chemical resistance (~25–50 μg cm^{-2}) and low total conductivity (~2×10^{-18} S cm^{-1} for GK_0) making the materials suitable for a number of practical applications [31].

To deepen the study of the structure of LD glasses the role of Al_2O_3 in Li_2O–SiO_2 glasses needs to be further clarified. Accordingly, the main objective of this work is to evaluate the effect of Al_2O_3 on the structure, properties and phase formation in glasses of 3 different systems: (i) Li_2O–SiO_2; (ii) Li_2O–Al_2O_3–SiO_2; (iii) and Li_2O–K_2O–Al_2O_3–SiO_2. Solid state magic angle spinning nuclear magnetic resonance (MAS-NMR) was employed to provide information on the local environment of silicon and aluminium in experimental glasses. The sintering behaviour and properties of the corresponding glass powder compacts was also a target subject during this study, in particular using a hot stage microscopy technique.

2. Experimental procedure

2.1. Glass preparation

Table 1 presents the detailed compositions of the experimental glasses along with their corresponding SiO_2/Li_2O ratios. A total of 9 glasses divided into 3 groups namely A, B and C belonging to the Li_2O–SiO_2, Li_2O–Al_2O_3–SiO_2 and Li_2O–K_2O–Al_2O_3–SiO_2 system, respectively, were synthesised. Compositions of group B were prepared from the A series by replacing SiO_2 with Al_2O_3. In group C glasses (similar to those investigated in the study [28]) composition C1

derived from B1 by replacing Li_2O by K_2O while C2 and C3 were obtained via increment of K_2O concentration at the expense of SiO_2. Powders of technical grade SiO_2 (purity $>99.5\%$) and of reactive grade Al_2O_3, Li_2CO_3, and K_2CO_3 were used. Homogeneous mixtures of batches (~100 g), obtained by ball milling, were calcined at 800 °C for 1 h and then melted in Pt crucibles at 1550 °C for 1 h, in air. All the glasses were produced in bulk by pouring glass melts on bronze mould in two different sets: the glasses of one set were immediately annealed at 450 °C for 1 h while the other set of glasses was kept in air to be preserved in the non-annealed condition. Additionally, glass frits were produced by quenching the melt in cold water. The obtained frits were dried and milled in a high-speed agate mill. The mean particle size of the glass powders as determined by light scattering technique (Beckman Coulter LS 230, CA USA; Fraunhofer optical model) was about 5–10 μm.

2.2. Thermo-physical properties of glasses

Non-annealed glass samples with particle sizes in the range of 500–1000 μm (collected by sieving of crushed non-annealed glass blocks) and weighing 40 mg were contained in an alumina crucible (the reference material was α-alumina powder) to perform differential thermal analysis (DTA, Setaram Labsys, Setaram Instrumentation, Caluire, France) in order to evaluate the glass transition temperature T_g, the crystallization onset temperature, T_c and peak temperature of crystallization, T_p ($\beta = 20$ K min^{-1}).

The coefficient of thermal expansion (CTE) of the annealed glasses was measured by dilatometry using prismatic samples of bulk glasses with cross section of 3×4 mm^2 (Bahr Thermo Analyse DIL 801 L, Germany; heating rate 5 K min^{-1}).

Archimedes' method (*i.e.* immersion in ethylene glycol) was employed to measure the apparent density of the bulk annealed glasses which was further applied along with compositions of glasses to calculate their excess volume (V_e) according to a procedure described elsewhere [30].

2.3. Structural characterization of glasses

^{29}Si MAS-NMR spectra were recorded on a Bruker ASX 400 spectrometer operating at 79.52 MHz (9.4 T) using a 7 mm probe at a spinning rate of 5 kHz. The pulse length was 2 μs and 60 s delay time was used. Kaolinite was used as the chemical shift reference. ^{27}Al MAS-NMR spectra were recorded on a Bruker ASX 400 spectrometer operating at 104.28 MHz (9.4 T) using a 4 mm probe at a spinning rate of 15 kHz. The pulse length was 0.6 μs and 4 s delay time was used. $Al(NO_3)_3$ was used as the chemical shift reference. The Q^n distributions were obtained by curve fitting and spectral deconvolution using DMFIT programme (version 2011) [32].

2.4. Crystalline phase analysis and microstructural evolution in glass–ceramics

Bulk parallelepiped glass samples were non-isothermally heat treated at 600, 700, 800 and 900 °C for 1 h, at a heating rate of 2 K min^{-1}. Glass powder compacts were heat treated at 800, 850 and 900 °C for 1 h at the heating rate of 2 K min^{-1}. The amorphous nature of the parent glasses and the nature of crystalline phases present in the glass–ceramics were determined by X-ray diffraction (XRD) analysis (Rigaku Geigerflex D/Mac, C Series, Japan; Cu K_a radiation, 2θ between 10° and 60° with a 2θ-step of 0.02 deg s^{-1}). The crystalline phases were identified by comparing the obtained diffractograms with patterns of standards complied by the International Centre for Diffraction Data (ICDD).

Archimedes' method was employed to measure the apparent density of the sintered glass-powder compacts. Microstructure observations were done at polished (mirror finishing) and then etched surfaces of samples (by immersion in 2 vol% HF solution for 2 min) by field emission scanning electron microscopy (SEM, Hitachi SU-70, Japan) under secondary electron mode.

2.5. Sintering and crystallization of glass powder compacts

A side-view hot-stage microscope (HSM, Leitz Wetzlar, Germany) equipped with a Pixera video-camera and image analysis system was used to investigate the sintering behaviour of glass powder compacts. The cylindrical shaped samples from glass powder compacts with height and diameter of ~3 mm were prepared by cold-pressing the glass powders. The cylindrical samples were placed on a $10 \times 15 \times 1$ mm^3 alumina (>99.5 wt% Al_2O_3) support and the measurements were conducted in air with a heating rate (β) of 5 K min^{-1}. The temperature was measured with a chromel–alumel thermocouple contacted under the alumina support. The temperatures corresponding to the characteristic viscosity points (first shrinkage (T_{FS}), maximum shrinkage (T_{MS}), softening (T_D), half ball (T_{HB}) and flow (T_F)) were obtained from the graphs and photomicrographs taken during the hot-stage microscopy experiment [33].

Apart from HSM investigation, the sintering process was explored using non-isothermal heat treatment of glass-powder compacts. Rectangular bars ($4 \times 5 \times 50$ mm^3) prepared by uniaxial pressing (80 MPa) were sintered at 800, 850 and 900 °C for 1 h. A heating rate of 2 K min^{-1} was maintained in order to prevent deformation of the samples.

3. Results

3.1. Casting ability and microstructure of glasses

Melting at 1550 °C for 1 h was adequate to obtain bubble-free homogenous glasses from all the investigated compositions. The absence of any crystalline inclusions was confirmed by XRD and SEM analyses (not shown). Cloudy appearance was characteristic only of A1, while no evidences of opacity in the other non-annealed glasses was detected by naked eye. The SEM images of as cast non-annealed samples (Fig. 1) revealed nanosized droplet phase embedded in the glass matrix suggesting occurrence of liquid–liquid phase separation in all investigated glasses. The droplet size and density distribution

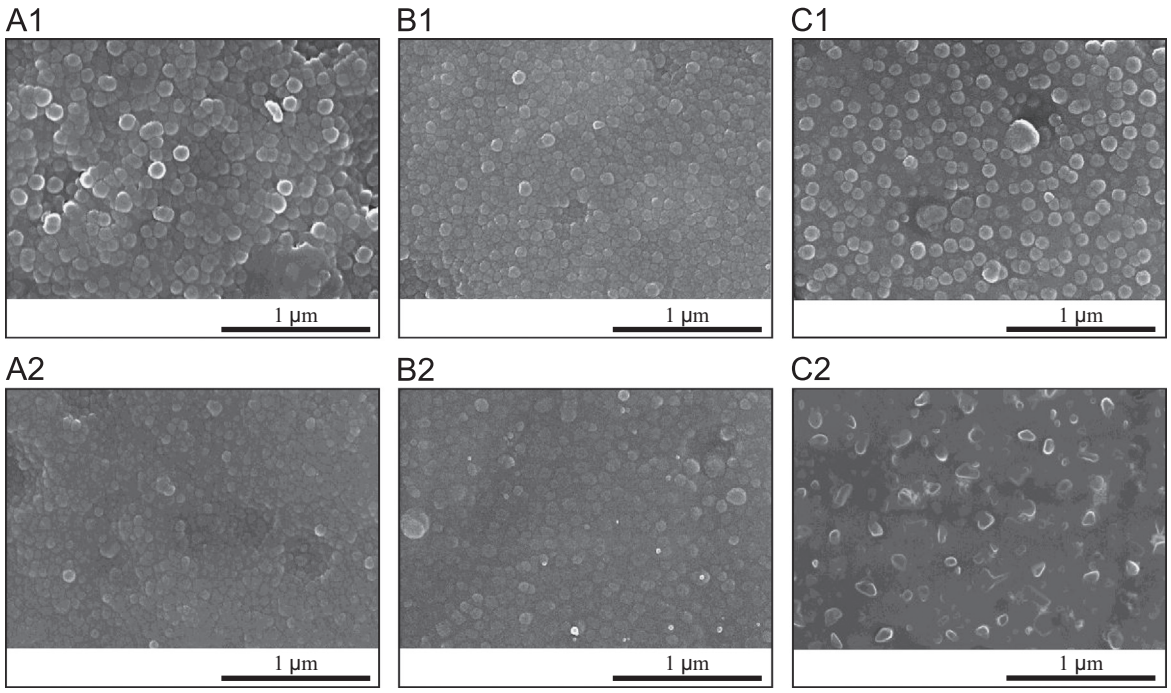

Fig. 1. SEM images of the experimental non-annealed bulk glasses (etched with 2 vol% HF solution for 1 min).

Table 2
Thermo-physical properties of the experimental glasses.

Glass	d (g cm^{-3})	V_e (cm^3 mol^{-1})	NBO/T	CTE $\pm$ 0.1 (10^{-6} K^{-1})	$T_g \pm 2$ (°C)	$T_c \pm 2$ (°C)	$T_c - T_g$ (°C)	$T_p \pm 2$ (°C)
A1	2.32 $\pm$ 0.03	1.05 $\pm$ 0.03	0.72	9.9	498	587	89	737
A2	2.33 $\pm$ 0.01	0.90 $\pm$ 0.03	0.78	10.8	495	606	111	733
A3	2.35 $\pm$ 0.04	0.66 $\pm$ 0.03	0.88	11.1	491	612	121	717
B1	2.36 $\pm$ 0.01	1.17 $\pm$ 0.01	0.63	9.6	504	662	158	781
B2	2.36 $\pm$ 0.04	1.08 $\pm$ 0.04	0.68	10.6	500	639	139	773
B3	2.37 $\pm$ 0.02	0.92 $\pm$ 0.02	0.78	11.7	495	620	117	746
C1	2.37 $\pm$ 0.01	1.08 $\pm$ 0.04	0.63	11.5	503	695	192	806
C2	2.38 $\pm$ 0.01	0.97 $\pm$ 0.05	0.68	11.5	500	663	163	800
C3	2.40 $\pm$ 0.01	0.76 $\pm$ 0.04	0.78	12.7	496	658	162	778

seemingly decreased from glass A1 to A3 (series A) and from glass B1 to B3 (series B) while increased from C1 to C3 in series C.

3.2. Structure and thermo-physical properties of glasses

3.2.1. Density, excess molar volume and thermal properties

The density values of glasses varied in the range 2.32–2.40 g cm^{-3} (Table 2). The observed general trend indicates that density increases in the sequence C > B > A and, consequently, glasses from the Li_2O–K_2O–Al_2O_3–SiO_2 system featured the highest density (2.37–2.40 g cm^{-3}) while the binary (Li_2O–SiO_2) glasses are the less dense ones (2.32–2.35 g cm^{-3}). Density increments with addition of Al_2O_3 (density ~4.00 g cm^{-3}) were expected assuming additive properties argument. But the same reasoning seems to fail when decreasing SiO_2/Li_2O and SiO_2/K_2O ratios. This might be explained considering the decreasing trend observed in the excess molar volume (V_e) of the glasses (Table 2). Assuming that sizes of Li and K cations are smaller than interstices their attraction to oxygen ion might cause decrease in the interstices' size [33,34]. In particular, Li ions actually compact the structure enough to offset their lower atomic mass, while K ions expand the structure, but not enough to offset their increase in atomic mass – relative to Si in each case.

The coefficient of thermal expansion (CTE) values of the glasses followed the sequence C > B > A (Table 2). Accordingly, within each group, the CTE increased upon decreasing of SiO_2/Li_2O or SiO_2/K_2O ratios (*e.g.* C3 > C2 > C1). The experimentally obtained trends are in good agreement with the CTE values calculated using a linear model of Appen that considers additive thermal expansion properties of oxides [35].

The DTA plots of glasses with a heating rate (β) of 20 K min^{-1} (Fig. 2) revealed well-defined features comprising

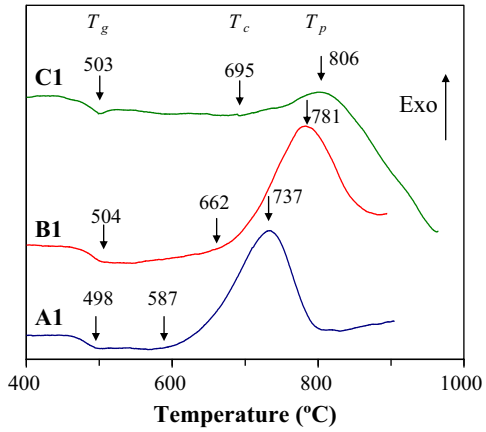

Fig. 2. DTA of glasses A1, B1 and C1.

endothermic and exothermic peaks from which transition point (T_g), temperature of onset crystallization (T_c) and peak temperature of crystallization (T_p), were determined (Table 2). General decreasing trends of T_c and T_p with decreasing the SiO_2/Li_2O ratio can be depicted from data reported in Table 2 and, being accompanied by a similar variation trend of T_g in each group. The observed lowering of T_g is in accordance with the calculated increasing number of non-bridging oxygens per tetrahedron (NBO/T) further supporting the hypothesis of depolymerisation of the glass network.

3.2.2. Structure analysis by MAS-NMR

^{29}Si MAS-NMR spectra of the experimental glasses feature broad bands, denoting the amorphous nature of these materials [36]. As expected depolymerisation trends were revealed in each series upon increasing modifier oxides (Li_2O, K_2O) concentration that correlates with calculated NBO/T numbers (Table 2). Likewise redistribution of silicon atoms occurs upon introducing of small amount of alumina in the binary Li_2O–SiO_2 system. This feature can be revealed from Fig. 3 demonstrating ^{29}Si MAS-NMR spectra of A1, B1 and C1 glasses. As a matter of fact, in the binary Li_2O–SiO_2 system Si atoms are distributed among Q^3 and Q^4 species whilst with addition of 2.63 mol% alumina those become localised in less polymerized Q^2 units. Considering the fact that the fraction of Q^4 species is almost unaffected (Fig. 3), Q^2 units in B1 glass apparently appeared at the expense of Q^3 groups. In the contrast, the formation of Q^2 units was suppressed in glass C1 which was derived from glass B1 by partial substituting of K_2O for Li_2O. Such development would result in the repolymerisation of glass network.

^{27}Al MAS-NMR spectra of glasses from series B and C are shown in Fig. 4. Comparison of the spectra revealed that B series glasses demonstrate ^{27}Al chemical shift towards lower values. In particular, spectra indicate increasing coordination numbers, Al[5] and Al[6], in detriment of Al[4], [37–39]. This suggests the dual role of Al_2O_3 as network former and modifier oxide in the Li_2O–Al_2O_3–SiO_2 system.

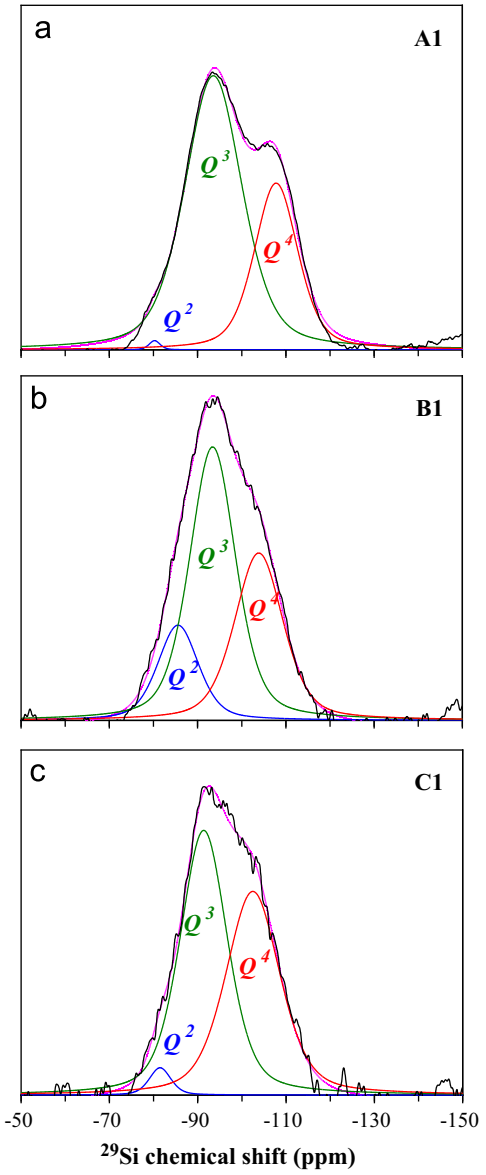

Fig. 3. ^{29}Si MAS-NMR spectra of glasses: (a) A1, (b) B1 and (c) C1. Dashed curves show the spectral deconvolution components used for fitting the data.

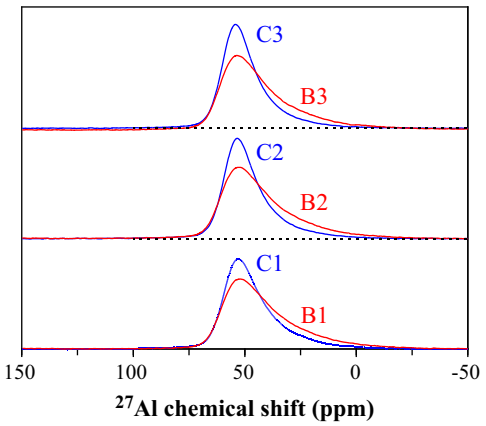

Fig. 4. ^{27}Al MAS-NMR spectra of glasses of series B and C.

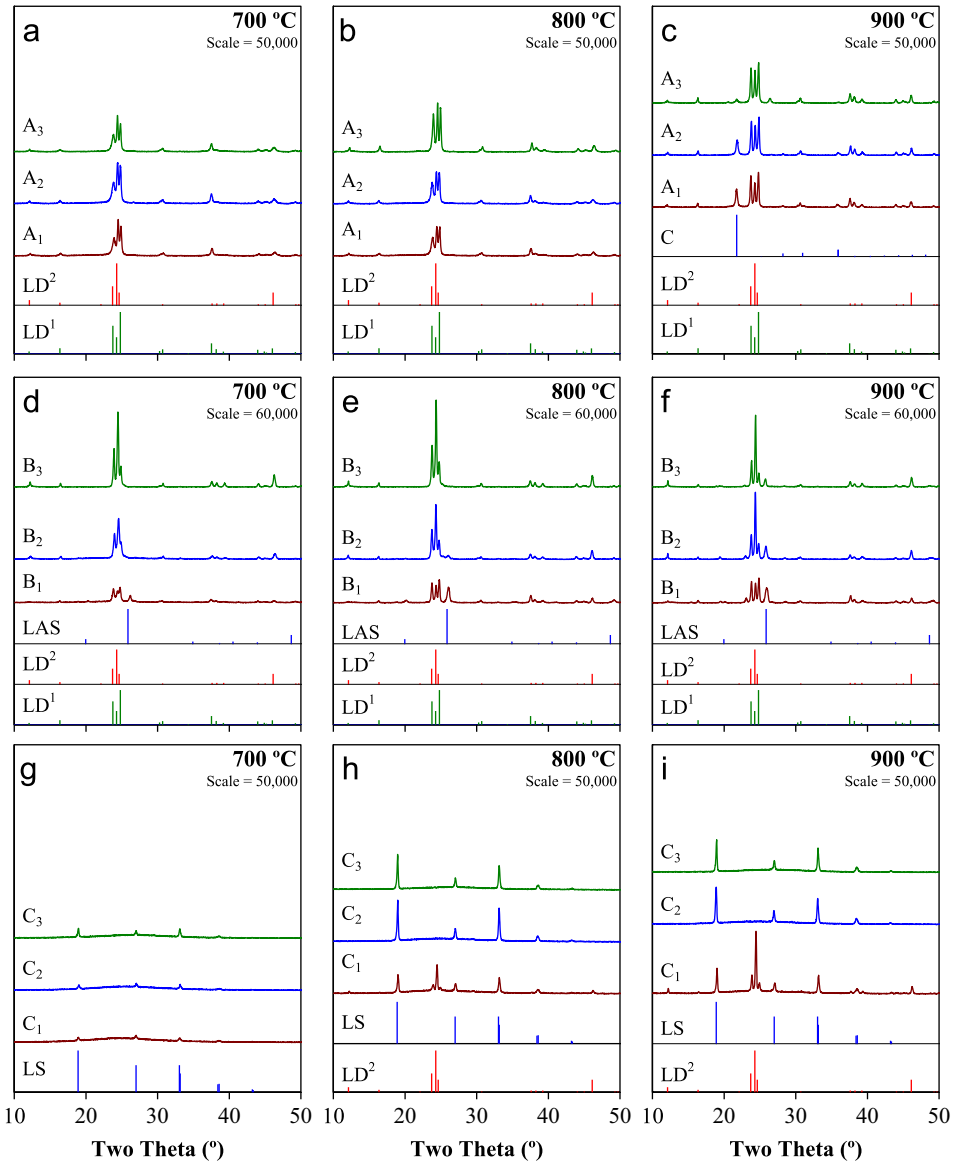

Fig. 5. X-ray diffractograms of experimental bulk glasses after heat treatment at different temperatures for 1 h. LS: lithium silicate (Li_2SiO_3, ICCD card 01-029-0828); LD^1: lithium disilicate ($Li_2Si_2O_5$, ICCD card 00-072-0102); LD^2: lithium disilicate ($Li_2Si_2O_5$, ICCD card 00-015-0637); LAS: virgilite ($Li_xAl_xSi_{3-x}O_6$, ICCD card 00-031-0707).

3.3. Crystallization behaviour of bulk glasses

3.3.1. Phase assemblage

All the investigated glass compositions were amorphous after heat treatment at 600 °C. Fig. 5(a–i), presents the X-ray diffractograms of the investigated bulk glasses heat treated within the temperature interval of 700–900 °C. LD was recorded as the single crystalline phase in the glasses of A series at 700 °C and 800 °C (Fig. 5(a, b)). The intensity of the peaks of LD slightly increased with the rising temperature and traces of cristobalite appeared at 900 °C (Fig. 5(c)). The addition of Al_2O_3 in the Li_2O–SiO_2 system enhanced the intensity of LD peaks and the formation of lithium aluminium silicate ($LiAlSi_2O_6$—LAS) (Fig. 5(d–f)). On the other hand, earlier studies [28,31] demonstrated that adding an excessive amount of K_2O tends to suppress the crystallization of LD and to promote the formation of LMS due to its lower activation energy for crystallization in comparison to LD [40,41]. Moreover, adding alkali oxides to silicate glasses decreases the melt viscosity, increases the fraction of NBO and enhances the tendency of the glass towards devitrification [42]. Indeed, in the C series, LD was formed only in the composition C1 with the lowest K_2O content [28,31].

3.3.2. Microstructure

Figs. 6–8 compare the SEM micrographs of A and B series of glasses heat treated at different temperatures. Etching with 2 vol% HF solution leads to serious dissolution of both crystal and amorphous phase. In the temperature interval 600–700 °C the small droplets underwent coalescence into bigger agglomerates at a rate that was higher in B series. This might be related to the conversation from the initial droplet/matrix

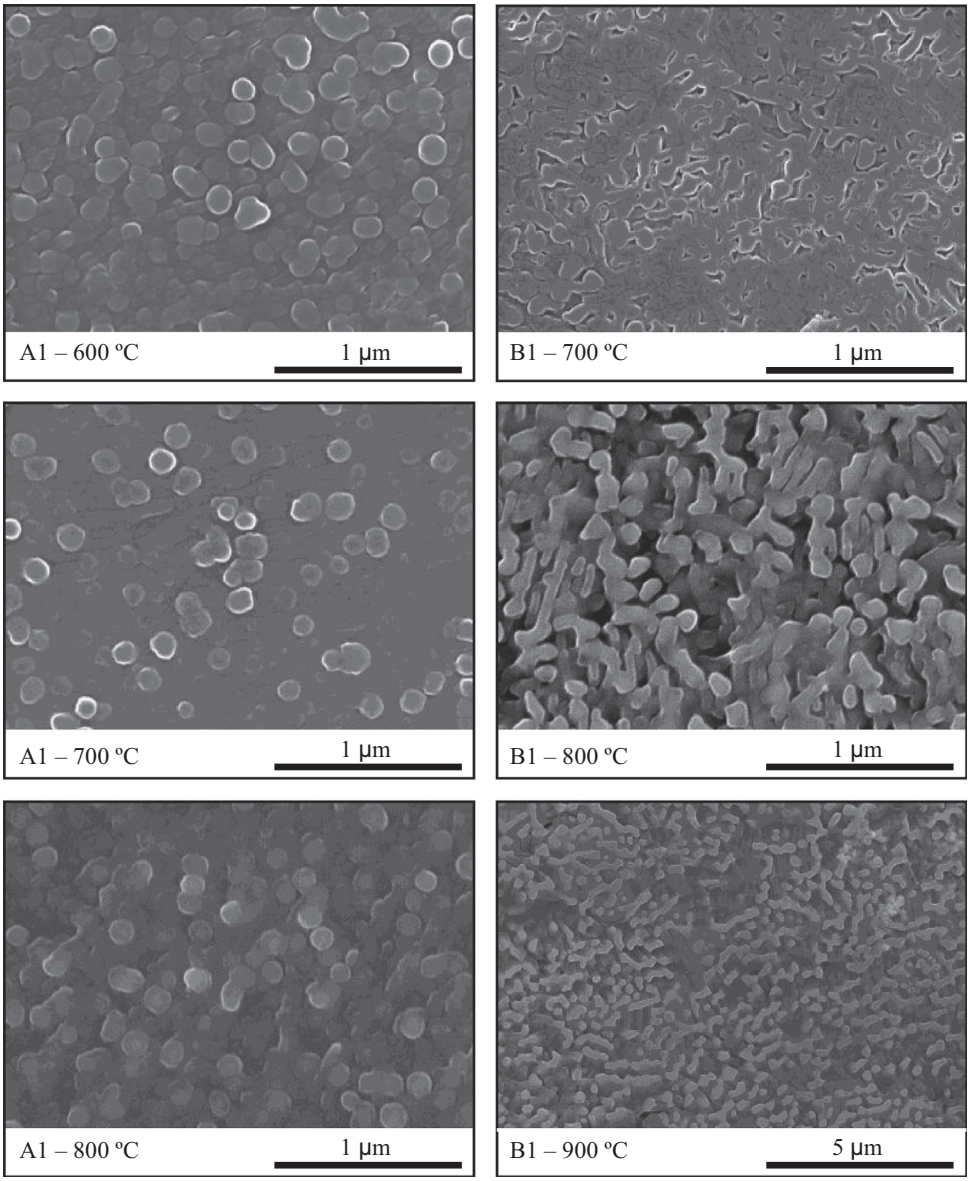

Fig. 6. SEM images of bulk glasses series A1 and B1 heat treated at 700, 800 and 900 °C for 1 h (etched with 2 vol% HF solution for 2 min).

structure to an interconnected structure that seemingly occurs upon heating of B series glasses. Simultaneously, LD crystals start to precipitate at 700 °C, being more evident in B series, which can be seen from corresponding XRD patterns (Fig. 5). Bulk glasses of series A and B exhibited ability towards bulk nucleation and crystallization of LD whilst glasses of series C were prone to surface crystallization. Formation of dendritic crystals characteristic for LMS [28] can be clearly observed in the C samples heat treated at 800 °C. In general, a dissolution rate in the lithium silicate system appreciably increases in the following gap LMS (cryst.) > LD (cryst.) > LD (glass) > quartz glass [2]. This observation pointed clearly that in glasses of C series at 900 °C LMS was first selectively etched out by HF acid before LD and glassy phase went into solution [28].

3.4. Sintering and crystallization of glass powder compacts

3.4.1. Sintering process

The experimental compositions from series A and B exhibited poor densification ability and resulted in porous and brittle samples, contrasting with the glass-powder compacts from series C that could be densely sintered [31]. In particular, samples from the binary system (series A) were extremely fragile. The incorporation of Al_2O_3 enhanced the sintering ability but not in desired extent to get proper densification. Samples of the different series heat treated at 900 °C for 1 h showed the following bending strength values: 2.40 ± 0.3 MPa (A1), 7.40 ± 0.6 MPa (B1) and 201 ± 16.0 MPa (C1). These considerable differences reflect the great importance of selecting the proper doses of both oxides (Al_2O_3 and K_2O) in order tune the densification ability

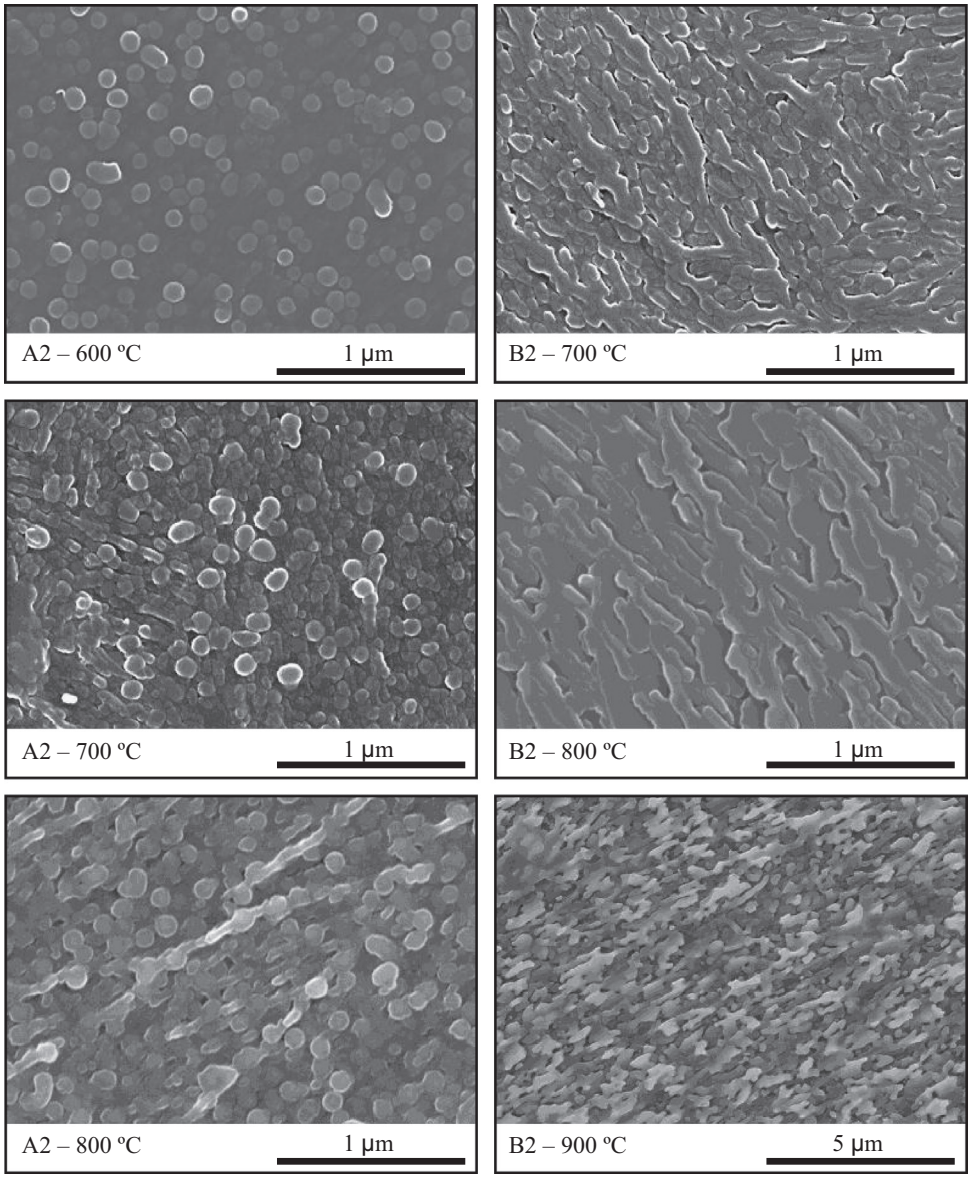

Fig. 7. SEM images of bulk glasses A2 and B2 heat treated at 700, 800 and 900 °C for 1 h (etched with 2 vol% HF solution for 2 min).

and the final properties of the sintered glass powder compacts in the present systems.

The HSM curves of the glass powder compacts of series A, B and C plotted in Fig. 9 show that densification generally occurs through viscous flow at temperatures slightly higher than T_g and dense materials are produced when the sintering process is completed before crystallization begins [36]. The glasses of series B exhibit just a single and small sintering step corresponding to a shrinkage volume of about 6–8%, while glasses of series C present two steps of sintering and a total variation of A/A_0 close to 0.60, *i.e.* a volume shrinkage of about 40%, corresponding to practically full densification [36].

The observed changes in the profiles of the samples A3, B3 and C3 during sintering (Fig. 10) reveal that the characteristic temperatures corresponding to softening (T_D), half ball (T_{HB}) and flow (T_F) for the Li_2O–K_2O–Al_2O_3–SiO_2 (C) system were reached significantly earlier in comparison to those observed in the Li_2O–SiO_2 and Li_2O–Al_2O_3–SiO_2 system. Moreover, in the glasses belonging to former systems sintering was completely retarded followed by abrupt dimensions changed at temperatures close to incongruent melting of LD.

4. Discussion

The phenomenon of amorphous phase separation in glasses has become an important topic of glass research since the fundamental investigations of Dietzel at the beginning of the 1940s [43]. It is a common phenomenon in silicate glasses that results in a heterogeneous mixture of two immiscible amorphous phases [1,3,43,44]. Dietzel explained this phenomenon on the basic field strength consideration [3,43]. Thus, in case of cooling binary silicates both cations compete for the oxygen

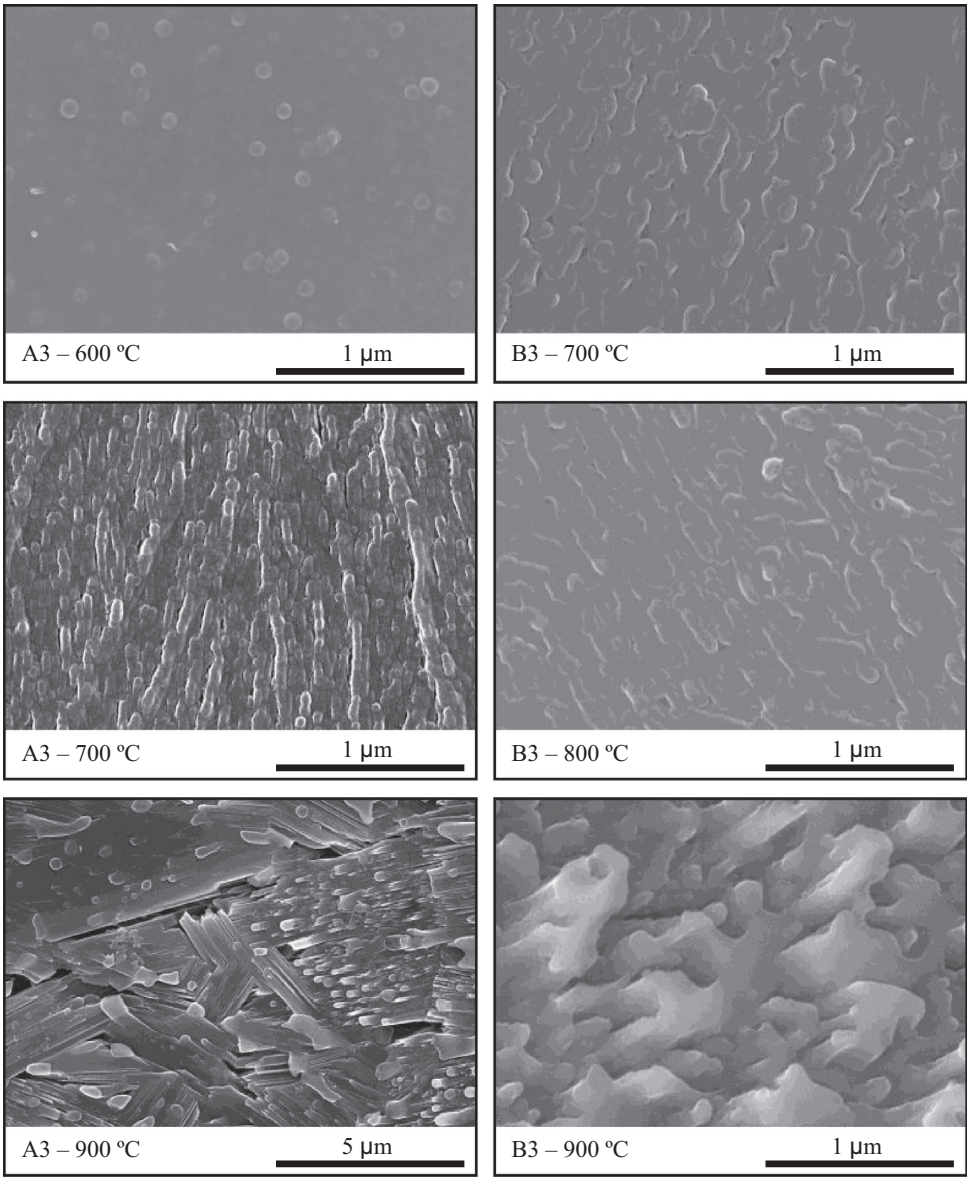

Fig. 8. SEM images of bulk glasses A3 and B3 heat treated at 700, 800 and 900 °C for 1 h (etched with 2 vol% HF solution for 2 min).

ions so as to surround themselves with the closest possible packing. When the field strengths of both cations are the same dissociation into two separate pure oxide phases often occurs. Below the solidus temperature, glass immiscibility is called a metastable phase separation and above that temperature it is called a stable one [44]. Among different types of alkali silicate glasses, lithium silicate glasses have the widest immiscibility range, between pure SiO_2 and close to $Li_2O \cdot 2SiO_2$ [3,43,44]. The viscosity of the melt at metastable immiscibility region is respectively higher and the mass transport will occur at slower rate [44], *i.e.* viscosity has a major factor effect on the kinetics of metastable phase separation. Apart of that, thermodynamic factors should be also considered along with the quench rate that causes the progress of separation into different phases. To make effort for understanding this phenomenon in the 3 different systems studied in the present work it is essential knowing the fact that the phase separation may be effective in increasing the driving force for precipitation of the crystalline phases [45].

With respect to the role of the modifier ions the results obtained in the present work are well correlated with the data reported by Schramm et al. [46] who investigated the extent of Q^n distributions for LD glasses in the composition region between 15 and 40 mol% Li_2O: the percentage of Q^4 decreased with increasing amounts of Li_2O, that of Q^3 reached a maximum at 30 mol% Li_2O, and the percentage of Q^2 showed tendency to grow at higher Li_2O concentrations. As for the role of alumina it is well known that this oxide suppresses the immiscibility temperature in many systems, eliminating any visible evidence of immiscibility [45]. Thus, in alkali–alkaline earth aluminosilicate glasses where the alumina to modifier oxide concentration ratio is less than one, addition of alumina

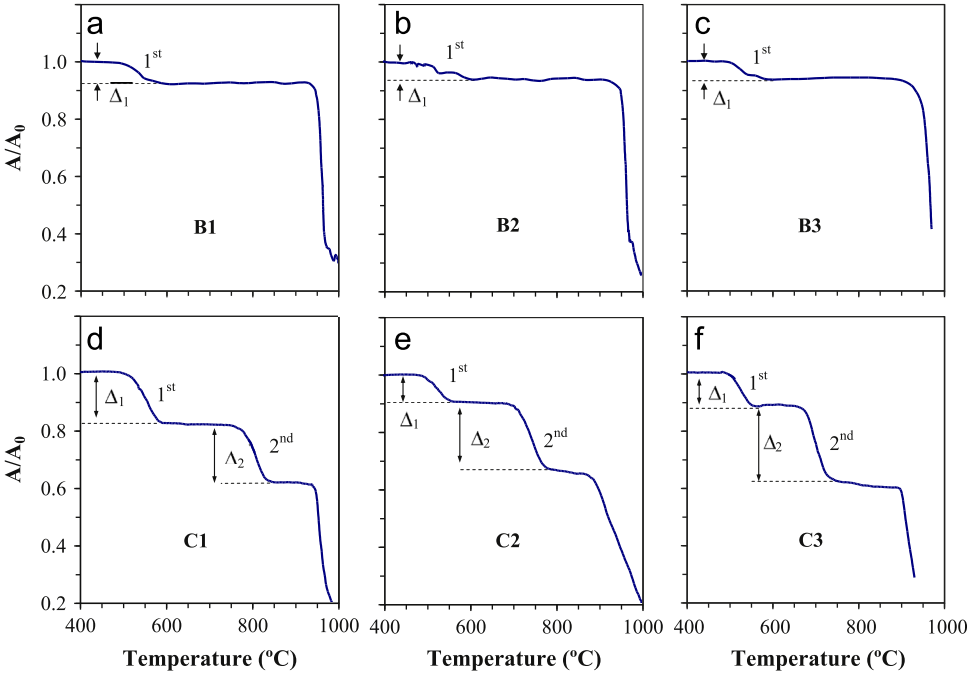

Fig. 9. HSM curves for glass-powders: (a) B1, (b) B2, (c) B3, (d) C1, (e) C2 and (f) C3.

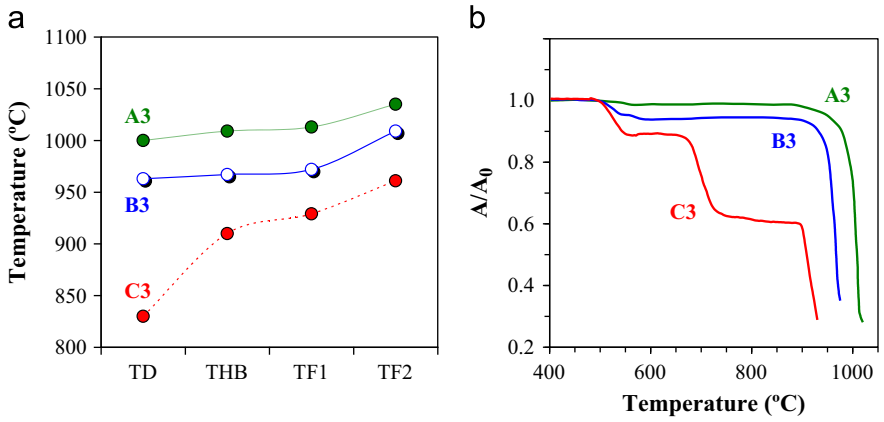

Fig. 10. HSM results for glasses A3, B3 and C3: (a) temperature parameters [softening (T_D), half ball (T_{HB}) and flow (T_F)] and (b) HSM curves.

would result in the replacement of Q^3 by groups Q^4, *i.e.* in increase of the connectivity number [1]. However, according to the results obtained adding Al_2O_3 to the Li_2O–SiO_2 binary system caused decrease in Q^3 units and increase of Q^2 units (Fig. 3). These structural changes are consistent with enhancing a glass network modifier role of Al_2O_3 in Li_2O–SiO_2 system. It is well known that to strengthen the glass network aluminium should be four-coordinated and each tetrahedral unit should be associated with a cation in its vicinity in order to maintain local charge neutrality of the $(AlO_{4/2})^-$ units. This scenario is valid for the C series glasses where charge neutrality is assured by the presence of K_2O [28,29,31]. However, in K_2O-free glasses of series B (Li_2O–Al_2O_3–SiO_2), aluminium tends partially to appear in five- or six-coordinate aluminium species, which would result in depolymerising of the glass network. This can be due to a large fraction of lithium cations captured in the Li-rich droplet phase leaving the remaining lithium content at the silica rich matrix being insufficient to satisfy the neutrality of the $(AlO_{4/2})^-$ units and an amount of Al^{3+} equivalent to that in excess over the metal cation content will become a network modifier. The higher coordination number of Al is well supported by the ^{27}Al MAS-NMR spectra of compositions B and C (Fig. 4), namely by the ^{27}Al chemical shifts of B glasses to lower values in comparison to those of group C glasses.

The structural features of the glasses affect the formation of crystalline phases. For instance, heat treating Al_2O_3-dopped bulk glasses of B series resulted in precipitation of LD as the major crystalline phase and LAS as the minor phase (Fig. 5(d–f)). The formation of LAS that should be favoured by six coordinated aluminium supports NMR results obtained from the Li_2O–Al_2O_3–SiO_2 glasses. On the other hand, the preferential formation of LMS in C series of glasses was already explained [27–29] using the model of Bischoff et al. and ^{29}Si

MAS-NMR results [47]. Moreover, earlier it was postulated that K_2O favoured the formation of LMS in preference to the LD [48].

Recently, a crystallization kinetics study of the glasses in the Li_2O–SiO_2, Li_2O–Al_2O_3–SiO_2 and Li_2O–K_2O–Al_2O_3–SiO_2 systems [49] revealed that glasses comprising Al_2O_3 and K_2O present the lower crystallization propensity, *i.e.* earlier crystallization and higher crystallization rate were observed in the Li_2O–Al_2O_3–SiO_2 and Li_2O–SiO_2 systems compared to the Li_2O–K_2O–Al_2O_3–SiO_2 glasses. Additionally, the lower T_c and T_p values of glasses from A and B series in comparison to those of C series (Table 2) meant that the crystallization process is delayed in C series glasses, while the resulting larger T_c–T_g differences favour densification of glass-powder compacts, a decisive factor to get strong glass–ceramics. This is in accordance with structural changes since ^{29}Si MAS-NMR data revealed repolymerization of the glass network after addition of both Al_2O_3 and K_2O to the Li_2O–SiO_2 system. Narrowing the T_c–T_g processing window in the less polymerised glass networks of series A and B (Fig. 3) compared to C completely hindered the densification of the glass powder compacts due the early LD formation (Fig. 2). Nevertheless, glass viscosity measurements should be performed to support the obtained results.

Regarding the sintering process of C series glasses only, the first step of densification was affected by crystallization. In composition C1 (lowest K_2O content), the first sintering step was separated by the temperature range where LMS was formed followed by a second sintering stage that occurred simultaneously with formation of LD phase [27–29]. This can be attributed to the formation of a more rigid glass network containing four coordinated $(AlO_{4/2})^-$ units and K^+ cations in its vicinity to maintain local charge neutrality. Therefore, a small addition of Al_2O_3 along with K_2O to pure Li_2O–SiO_2 system is crucial to promote glass stability against crystallization, enhance the densification behaviour and the ultimate mechanical strength. In the present study, beneficial effects of adding both Al_2O_3 and K_2O are only observed up to about 3 mol% of each oxide, being therefore a matter of process optimization [29].

5. Conclusions

The effect of Al_2O_3 and K_2O on structure, sintering and devitrification behaviour of glasses in the Li_2O–SiO_2 system along with the properties of the resultant glass–ceramics has been investigated. The results can be summarized in the following conclusions:

(1) The structure of A and C series of glasses consists predominantly of Q^3 and Q^4 units and the silicate glass network trends to depolymerise with decreasing SiO_2/Li_2O and SiO_2/K_2O ratios.
(2) The partial replacement of SiO_2 by Al_2O_3 in Li_2O–SiO_2 glasses (group B) enhanced the trend towards depolymerisation, reflected by increase in Q^2 at the expense of Q^3 units, with Al_2O_3 playing dual role of a glass network former and modifier. This latter role of Al_2O_3 in the Li_2O–Al_2O_3–SiO_2 system is supported by the analysis of ^{27}Al MAS-NMR spectra. All compositions of group B show ^{27}Al chemical shifts to lower values in comparison to glasses in group C, revealing increasing fractions of Al [5] and Al [6] in detriment of Al [4]. Moreover, crystallization of those glasses resulted in the formation of LD and LAS phases.
(3) The experimental compositions from series A and B exhibited poor densification ability resulted in porous samples of brittle nature, contrasting with well sintered glass-powder compacts from series C. This was due to the formation of a more rigid glass network in glasses of series C containing four coordinated $(AlO_{4/2})^-$ units and K^+ cations in its vicinity to maintain local charge neutrality. Therefore, a small addition of K_2O to pure Li_2O–Al_2O_3–SiO_2 system is crucial to enhance the densification behaviour and the ultimate mechanical strength.

Acknowledgements

Hugo R. Fernandes is grateful for the financial support of CICECO and for the Ph.D. Grant (SFRH/BD/41307/2007) from the FCT, Portugal.

References

[1] O.V. Mazurin, E.A. Porai-Koshits, Phase Separation in Glasses, North-Holland, Amsterdam, 1984.
[2] W. Vogel, Structure and Crystallization of Glasses, Pergamon Press, Leipzig, 1971.
[3] W. Vogel, in: Glass Chemistry, Springer, Berlin, 1994.
[4] M.H. Lewis, Glasses and Glass–Ceramics, Chapman and Hall, London, 1989.
[5] Z. Strnad, Glass Science and Technology, Elsevier, New York, 1986.
[6] A.R. West, Solid State Chemistry and its Applications, John Wiley and Sons, New York, 1984.
[7] W. Höland, G. Beall, Glass–Ceramic Technology, The American Ceramic Society, Westerville, Ohio, 2002.
[8] J.M.G. Barrett, David L. Clark, F.L. Gainesville, Larry L. Hench, The Board of Regents, State of Florida, University of Florida, Tallahassee, FL, 1980 (U.S. Patent 4,189,325).
[9] J.M.T. Wu, T.W. Cannon, R. Warren, East Brunswick, NJ, Panzera, Carlino (Belle Mead, NJ) (Johnson & Johnson Dental Products Company (East Windsor, NJ), 1985.
[10] M. Bengisu, R.K. Brow, J.E. White, Interfacial reactions between lithium silicate glass–ceramics and Ni-based superalloys and the effect of heat treatment at elevated temperatures, Journal of Materials Science 39 (2) (2004) 605–618.
[11] M.P. Borom, A.M. Turkalo, R.H. Doremus, Strength and microstructure in lithium disilicate glass–ceramics, Journal of the American Ceramic Society 58 (9–10) (1975) 385–391.
[12] M. Goswami, G.P. Kothiyal, L. Montagne, L. Delevoye, MAS-NMR study of lithium zinc silicate glasses and glass–ceramics with various ZnO content 181 (2) (2008) 269–275 Journal of Solid State Chemistry 181 (2) (2008) 269–275.
[13] M. Guazzato, M. Albakry, S.P. Ringer, M.V. Swain, Strength, fracture toughness and microstructure of a selection of all-ceramic materials.

Part I. Pressable and alumina glass-infiltrated ceramics, Dental Materials 20 (5) (2004) 441–448.
[14] W. Höland, E. Apel, C. van Hoen, V. Rheinberger, Studies of crystal phase formations in high-strength lithium disilicate glass-ceramics, Journal of Non-Crystalline Solids 352 (38–39) (2006) 4041–4050.
[15] Y. Iqbal, W.E. Lee, D. Holland, P.F. James, Metastable phase formation in the early stage crystallisation of lithium disilicate glass, Journal of Non-Crystalline Solids 224 (1) (1998) 1–16.
[16] G. Beall, Design of glass–ceramics, Solid State Science 3 (1989) 333–354.
[17] G. Beall, Glass–ceramics: recent developments and application, Ceramic Transactions 30 (1993) 241–266.
[18] L.M. Echevería, New lithium disilicate glass–ceramics, Boletin da la Sociedad Espanola de Cerámica e Vidrio 5 (1992) 183–188.
[19] M. Schweiger, Microstructure and mechanical properties of a lithium disilicate glass–ceramic in the SiO_2–Li_2O–K_2O–ZnO–P_2O_5 system, Glastechnische Berichte-Glass Science and Technology 73 (2000) 43–50.
[20] C.S. von Clausbruch, M. Schweiger, W. Holand, V. Rheinberger, The effect of P_2O_5 on the crystallization and microstructure of glass–ceramics in the SiO_2–Li_2O–K_2O–ZnO–P_2O_5 system, Journal of Non-Crystalline Solids 263 (1–4) (2000) 388–394.
[21] M. Frank, M. Schweiger, V. Rheinberger, W. Höland, High-strength translucent sintered glass–ceramics for dental application, Glastechnische Berichte-Glass Science and Technology 71C (1998) 345–348.
[22] W. Höland, Material Science Fundamentals of the IPS Empress 2 Glass–Ceramic, 12, 3–10 Ivoclar-Vivadent Report.
[23] W. Höland, M. Schweiger, M. Frank, V. Rheinberger, A comparison of the microstructure and properties of the IPS Empress®2 and the IPS Empress® glass–ceramics, Journal of Biomedical Materials Research 53 (4) (2000) 297–303.
[24] M. Schweiger, M. Frank, C.S. Von Clausbruch, W. Höland, V. Rheinberger, Microstructure and properties of pressed glass–ceramic core to zirconia, Quintessence Dental Technology 21 (1998) 73–79.
[25] K.D. Kim, Crystallization behavior during cooling and glass-forming ability of Al_2O_3-poor Li_2O–Al_2O_3–SiO_2 melts, Journal of Non-Crystalline Solids 354 (15–16) (2008) 1715–1720.
[26] S. Morimoto, Effect of K_2O on crystallization of Li_2O–SiO_2 glass, Journal of the Ceramic Society of Japan 114 (1326) (2006) 195–198.
[27] H.R. Fernandes, D.U. Tulyaganov, A. Goel, J.M.F. Ferreira, Structural characterisation and thermo-physical properties of glasses in the Li_2O–SiO_2–Al_2O_3–K_2O system, Journal of Thermal Analysis and Calorimetry 103 (3) (2011) 827–834.
[28] H.R. Fernandes, D.U. Tulyaganov, A. Goel, J.M.F. Ferreira, Effect of K_2O on structure-property relationships and phase transformations in Li_2O–SiO_2 glasses, Journal of the European Ceramic Society 32 (2) (2012) 291–298.
[29] H.R. Fernandes, D.U. Tulyaganov, A. Goel, M.J. Ribeiro, M.J. Pascual, J.M.F. Ferreira, Effect of Al_2O_3 and K_2O content on structure, properties and devitrification of glasses in the Li_2O–SiO_2 system, Journal of the European Ceramic Society 30 (10) (2010) 2017–2030.
[30] H.R. Fernandes, D.U. Tulyaganov, I.K. Goel, J.M.F. Ferreira, Crystallization process and some properties of Li_2O–SiO_2 glass–ceramics doped with Al_2O_3 and K_2O, Journal of the American Ceramic Society 91 (11) (2008) 3698–3703.
[31] H.R. Fernandes, D.U. Tulyaganov, M.J. Pascual, V.V. Kharton, A. A. Yaremchenko, J.M.F. Ferreira, The role of K_2O on sintering and crystallization of glass powder compacts in the Li_2O–K_2O–Al_2O_3–SiO_2 system, Journal of the European Ceramic Society 32 (2012) 2283–2292.
[32] D. Massiot, F. Fayon, M. Capron, I. King, S. Le Calvé, B. Alonso, J.O. Durand, B. Bujoli, Z. Gan, G. Hoatson, Modelling one- and two-dimensional solid-state NMR spectra, Magnetic Resonance in Chemistry 40 (2002) 70–76.
[33] C. Lara, M.J. Pascual, A. Duran, Glass-forming ability, sinterability and thermal properties in the systems RO–BaO–SiO_2 (R=Mg, Zn), Journal of Non-Crystalline Solids 348 (2004) 149–155.
[34] J.E. Shelby, Introduction to Glass Science and Technology, The Royal Society of Chemistry, Cambridge, 1997.
[35] A.I. Priven, General method for calculating the properties of oxide glasses and glass-forming melts from their composition and temperature, Glass Technology 45 (6) (2004) 244–254.
[36] J. Schneider, V.R. Mastelaro, H. Panepucci, E.D. Zanotto, ^{29}Si MAS-NMR studies of Q^n structural units in metasilicate glasses and their nucleating ability, Journal of Non-Crystalline Solids 273 (2000) 8–18.
[37] M.E. Smith, Application of ^{27}Al NMR techniques to structure determination in solids, Applied Magnetic Ressonance 4 (1993) 1–64.
[38] H. Oudadesse, A.C. Derrien, M. Lefloch, D. J., MAS-NMR studies of geopolymers heat-treated for applications in biomaterials field, Journal of Materials Science 42 (2007) 3092–3098.
[39] P.A. Wright, Microporous Framework Solids, Royal Society of Chemistry, London, 2007.
[40] W.F. Hammetter, R.E. Loehman, Crystallization kinetics of a complex lithium silicate glass-ceramic, Journal of the American Ceramic Society 70 (8) (1987) 577–582.
[41] A.P.N. Oliveira, O.E. Alarcon, T. Manfredini, G.C. Pellacani, C. Siligardi, Crystallisation kinetics of a $2.3Li_2O.1.1ZrO_2 6.6\ SiO_2$ glass, Physics and Chemistry of Glasses 41 (2) (2000) 100–103.
[42] H. Scholze, Glass: Nature, Structure and Properties, Springer, Berlin, 1991.
[43] A. Dietzel, Zusammenhänge zwischen Oberflächenspnnung und Struktur von Glasschmelzen, Kolloid-Z 100 (3) (1942) 368–380.
[44] D.R. Uhlmann, A.G. Kolbeck, Phase separation and revolution in concepts of glass structure, Physics and Chemistry of Glasses 17 (5) (1976) 146–158.
[45] A.M. Alper, Phase Diagrams: Materials Science and Technology, Academic Press, New York, 1970.
[46] C.M. Schramm, B.H.W.S. de Jong, V.E. Parzialet, ^{29}Si Magic Angle Spinning NMR study on local silicon environments in amorphous and crystalline lithium silicates, Journal of the American Ceramic Society 106 (1984) 4396–4402.
[47] C. Bischoff, H. Eckert, E. Apel, V.M. Rheinberger, W. Holand, Phase evolution in lithium disilicate glass–ceramics based on non-stoichiometric compositions of a multi-component system: structural studies by ^{29}Si single and double resonance solid state NMR, Physical Chemistry Chemical Physics 13 (2011) 4540–4551.
[48] P.W. McMillan, Glass–Ceramics, Academic Press, London, 1979.
[49] H.R. Fernandes, D.U. Tulyaganov, J.M.F. Ferreira, Al_2O_3/K_2O-containing non-stoichiometric lithium disilicate-based glasses—a study of crystallisation kinetics, Journal of Thermal Analysis and Calorimetry Published online (2012).